Quaternary Environments and Humans 2 (2024) 100044

Contents lists available at ScienceDirect

Quaternary Environments and Humans

journal homepage: www.journals.elsevier.com/quaternary-environments-and-humans

Constraining the age of the Middle Stone Age locality of Bargny (Senegal) through a combined OSL-ESR dating approach

E. Ben Arous [a,b,c,*], K. Niang [b,d], J.A. Blinkhorn [b,e], M. Del Val [a], A. Medialdea [a], C. Coussot [f,g], M.J. Alonso Escarza [a], M.D. Bateman [h], A. Churruca Clemente [a], A.F. Blackwood [b,i,j], J. Iglesias-Cibanal [a], C. Saíz [a], E.M.L. Scerri [b,k,l], M. Duval [a,i,m]

[a] Centro Nacional de Investigación sobre la Evolución Humana (CENIEH), Burgos, Spain
[b] Human Palaeosystems Group, Max Planck Institute of Geoanthropology, Jena, Germany
[c] Histoire naturelle de l'Homme préhistorique, Muséum national d'Histoire naturelle, Paris, France
[d] Département d'Histoire, Université Cheikh Anta Diop de Dakar, Dakar, Senegal
[e] Department of Archaeology, Classics and Egyptology, University of Liverpool, Liverpool, UK
[f] Laboratoire de Géographie Physique, UMR 8591 CNRS, Thiais, France
[g] Institut National de recherches Archéologiques Préventives, Centre archéologique de Chartres, Chartres, France
[h] University of Sheffield, Department of Geography, Sheffield, United Kingdom
[i] Palaeoscience Labs, Dept. Archaeology and History, La Trobe University, Melbourne Campus, Bundoora, Victoria, Australia
[j] Human Evolution Research Institute (HERI), Department of Geological Sciences, University of Cape Town, Cape Town, South Africa
[k] Department of Classics and Archaeology, University of Malta, Msida, Malta
[l] Department of Prehistory, University of Cologne, Cologne, Germany
[m] Australian Research Centre for Human Evolution (ARCHE), Griffith University, Brisbane, Australia

ARTICLE INFO

Handling Editor: Dr Zerboni Andrea

Keywords:
ESR dating
OSL dating
Middle Stone Age
West Africa
Quartz mineral

ABSTRACT

The Middle Stone Age (MSA) is the major chrono-cultural phase associated with the emergence and evolution of *Homo sapiens* in Africa. Despite its importance, the MSA has not been evenly investigated across Africa, and West Africa in particular remains poorly understood. Although new research is beginning to fill in this crucial gap of knowledge, the existing MSA chronologies in West Africa only rely on Optically Stimulated Luminescence (OSL) dating. In this context, the increasing use of a multi-method dating approach appears essential to strengthen this emerging geochronological framework. Here, we apply such approach to constrain the age of Bargny locality, located in close proximity to the modern Senegalese coast (South of Dakar), and which documents one of the oldest MSA occupations in West Africa. Specifically, we combine OSL and Electron Spin Resonance (ESR) methods to date the MSA sites of Bargny 3 (BG3) and Bargny 1 (BG1). A mean OSL age of 127±8 ka may be proposed for the MSA of BG3, which is in good agreement with a mean Ti-H ESR age of 125±14 ka from the same unit. Interestingly, similar ages are obtained by OSL (144±7 ka) and Ti-H ESR (138±14 ka) for the MSA horizon from BG1. While these results illustrate the great potential of the combined OSL-ESR dating approach to establish robust chronologies, they also contribute to improve the geographical and chronological resolution of the MSA record in West Africa. More specifically, they also corroborate the presence of MSA occupations along the Senegambian coast around the MIS 6-MIS 5 transition. In combination with the associated estuarine environments and mangrove forest, the evidence from Bargny adds to the known diversity, and likely complex behaviour, of early human populations living by Africa's coastlines.

1. Introduction

The earliest occurrence of Middle Stone Age (MSA) technologies dates to ~ 300 thousand years ago (ka) and is contemporaneous with the emergence of the *H. sapiens* clade (e.g., Brooks et al., 2018; Deino et al., 2018; Hublin et al., 2017; Richter et al., 2017). Although the MSA is a crucial cultural period that constitutes a major change in our species' evolutionary and cognitive history, vast swathes of Africa such as West

* Corresponding author at: Centro Nacional de Investigación sobre la Evolución Humana, Burgos, Spain.
E-mail addresses: ben-arous@gea.mpg.de, eslem.benarous@cenieh.es (E. Ben Arous).

https://doi.org/10.1016/j.qeh.2024.100044
Received 29 June 2024; Received in revised form 26 September 2024; Accepted 24 November 2024
Available online 26 November 2024

Africa, have seen less investment in research, in contrast to other regions of the continent (see Scerri et al., 2018 for discussion). This is the case for inland regions, as well as for coasts, which are thought to have been particularly favorable environments for early humans (e.g., Campmas, 2017; Will et al., 2016). In temperate northern and southern Africa, evidence for MSA occupation of the coastline is well documented in numerous cave sites, typically preserving not only rich stone tool assemblages, but also a wealth of information regarding subsistence patterns and exploitation of marine resources (e.g., Ben Arous et al., 2022; Campmas, 2017). In contrast, comparable evidence from tropical Africa is scarce, and probably best represented by MSA occupation from Panga ya Saidi in Kenya (Shipton et al., 2018).

Multidisciplinary investigations have recently been initiated to address the spatial and temporal knowledge gaps in West Africa. Over the last decade, archaeological investigations have revealed a probable late persistence of the MSA until the Pleistocene-Holocene boundary (Scerri, 2017; Scerri et al., 2021), with technological continuities stretching back through time to at least MIS 5e (Douze et al., 2021), and even to late MIS 6 (Niang et al., 2023). In other words, these investigations have shown a regional MSA sequence spanning from at least Marine Isotope Stage (MIS 6) until MIS 2 (~150–11 ka) and documenting a distinct regional cultural trajectory. In particular, evidence from continental sites in the current Sahelian savanna biome have also shown a significant technical diversity (e.g. debitage Levallois, discoid, bipolar; bifacial tools; use of the pressure technique) from the MIS 4 to MIS 2 (Chevrier et al., 2018; Lebrun et al., 2016; Schmid et al., 2021).

Since 2018, new investigations have begun to document the MSA of tropical Senegambian coastal sites (Niang et al., 2023, 2020), in order to understand past human interaction with coastal (or sub-coastal) environments in this region. In particular, two key localities are critical to this endeavor, Tiémassas and Bargny. Multiple MSA occupation horizons dated by Optically Stimulated Luminescence (OSL) to between 62 ±3 ka to 26±1 ka have been reported at Tiémassas 2 (Niang et al., 2020), while Bargny 1 documents the oldest yet-known dated MSA in West Africa, initially constrained to 150±6 ka using OSL (Niang et al., 2023). Critically, this dated occupation was associated with high-resolution palaeoecological studies, highlighting the estuarine context of the MSA at the site, and, for the first time, mangrove habitats. Importantly, investigations within this landscape have also led to the identification of another MSA site, Bargny 3, reinforcing thus the importance of Bargny locality for our understanding of MSA occupations of this coastline. Consequently, corroborating the existing chronological framework with additional dating results derived from different methods is crucial for consolidating and refining the timing of the West African MSA. This will facilitate comparisons with other regions of the continent, where multi-method dating programs are more frequently employed (Ben Arous et al., 2022; Caruana et al., 2023; Daujeard et al., 2020; Duval et al., 2021; Herries et al., 2009; Smith et al., 2018). However, applying such a dating approach to the West African MSA is also quite challenging. For example, the use of well-established numerical dating methods that are typically applied to MSA sites elsewhere in Africa, such as Radiocarbon, Uranium-series, or Argon-Argon, requires suitable materials (e.g., bones, charcoal, shells, calcite, volcanic minerals) that are often absent from West African sites. In contrast, quartz is a ubiquitous mineral, opening the possibility for a widespread application of trapped-charge dating methods such as Luminescence and Electron Spin Resonance (ESR). MSA occupations in the region have been traditionally dated using OSL (Lebrun et al., 2016; Niang et al., 2018; Rasse et al., 2020, 2012; Tribolo et al., 2010), while Infrared stimulated Luminescence (IRSL) dating has instead never been used due to intense tropical weathering, leading to the near or complete absence of feldspar preservation in the sedimentary record. Unlike OSL, the ESR method has comparatively never been used so far in West Africa, despite being applicable to the same quartz fraction as OSL, providing thus a very useful semi-independent age control. Following a combined OSL-ESR dating approach that has proven increasingly successful over the last few years (e.g., Bartz et al., 2019, 2018; Duval et al., 2022; Méndez-Quintas et al., 2018), we present here new dating results for Bargny 1, complementing the existing OSL chronology proposed by Niang et al. (2020), and for the new MSA site of Bargny 3.

2. Bargny

2.1. Context

Bargny limestone quarries are located ~30 km south of Dakar (Fig. 1). The presence of Stone Age lithic artefacts was first reported in 1941 and further excavations in 1975 have confirmed their preservation in stratigraphy > 25 cm thickness (Diop, 1976). Subsequent surveys and excavations have led to the identification of various open-air sites, including Bargny 1 and Bargny 3 (Niang et al., 2023). Bargny 1 has recently be presented and discussed in Niang et al. (2023). The stratigraphic sequence is made of six stratigraphic units number 1–6 from top to bottom, with limited evidence of later prehistoric archaeology in the uppermost Unit 1. Below this unit, three archaeologically-sterile horizons were identified (Units 2–4), followed below by a bright orange sand with gravels (Unit 5) containing a rich MSA assemblage, overlying an uneven weathering horizon (Unit 6) on top of the limestone bedrock (Niang et al., 2023). OSL dating of quartz minerals following the Single Aliquot Regeneration (SAR) procedure constrained Units 4–2 to the Late Pleistocene to early Holocene time range, while the MSA assemblage in Unit 5 was dated to 150±6 ka.

2.2. Bargny 3 sequence

New excavations were conducted at Bargny quarries in 2018 (Fig. 1) in direct response to the threat from quarrying of this important heritage resource in the Bargny landscape. Bargny 3 is located approximately 450 m in south-east of Bargny 1, with both sites exposed and accessible as a result of ongoing quarrying activities. Investigation of the archaeological deposits at Bargny 3, which spans a total surface of 72 m^2 (12 m*6 m, Fig. 1), was naturally divided into two discrete sectors (Sector 1 and 2) due to recent incision and reworking of the deposits. Disturbed deposits were not excavated. Both sectors showed a comparable stratigraphic sequence, and the deposits can be directly correlated to those previously observed at Bargny 1. In Sector 1, the uppermost deposit (Unit 1) is a ~30 cm thick dark brownish-grey silty sand preserving evidence of protohistoric occupation, including burials, ceramics, and marine shells, directly underlain by an archaeologically sterile mid-greyish brown silty sand (Unit 2; ~70 cm). The Unit 3 is a ~20 cm thick mid-greyish silty sand. The presence of carbonate powder and fine nodules increases within Unit 3 towards the base with more dense and larger carbonate nodules (5–10 mm diameter), with a sharp contact with underlying deposits. Unit 4 is composed by a pale brownish-grey silty sand, typically ~35 cm thick, with carbonates showing some lateral variability of facies and higher density closer to the limestone bedrock. The main archaeological horizon, Unit 5, is characterized by a ~45 cm thick orange silty sand with presence of ferre-gravels and some carbonates and associated with a large number of MSA lithic artefacts (n > 6000). Preliminary technological analysis shows that the artefact assemblage from Bargny 3 includes classic MSA technologies such as Levallois and discoidal reduction sequences and sparse retouched flake tools (Fig. 1). The lowermost deposit (Unit 6) is made of angular bedrock fragments supported by fine sediments similar to the fine orange sands from Unit 5 mixed with banded clays exposed in the underlying bedrock horizon. The apparent thickness of exposed bedrock locally reaches >1 m.

3. Material and methods

Six ESR/OSL sediment samples were collected from Bargny 3 by inserting opaque metal tubes into the sections. The sampling was

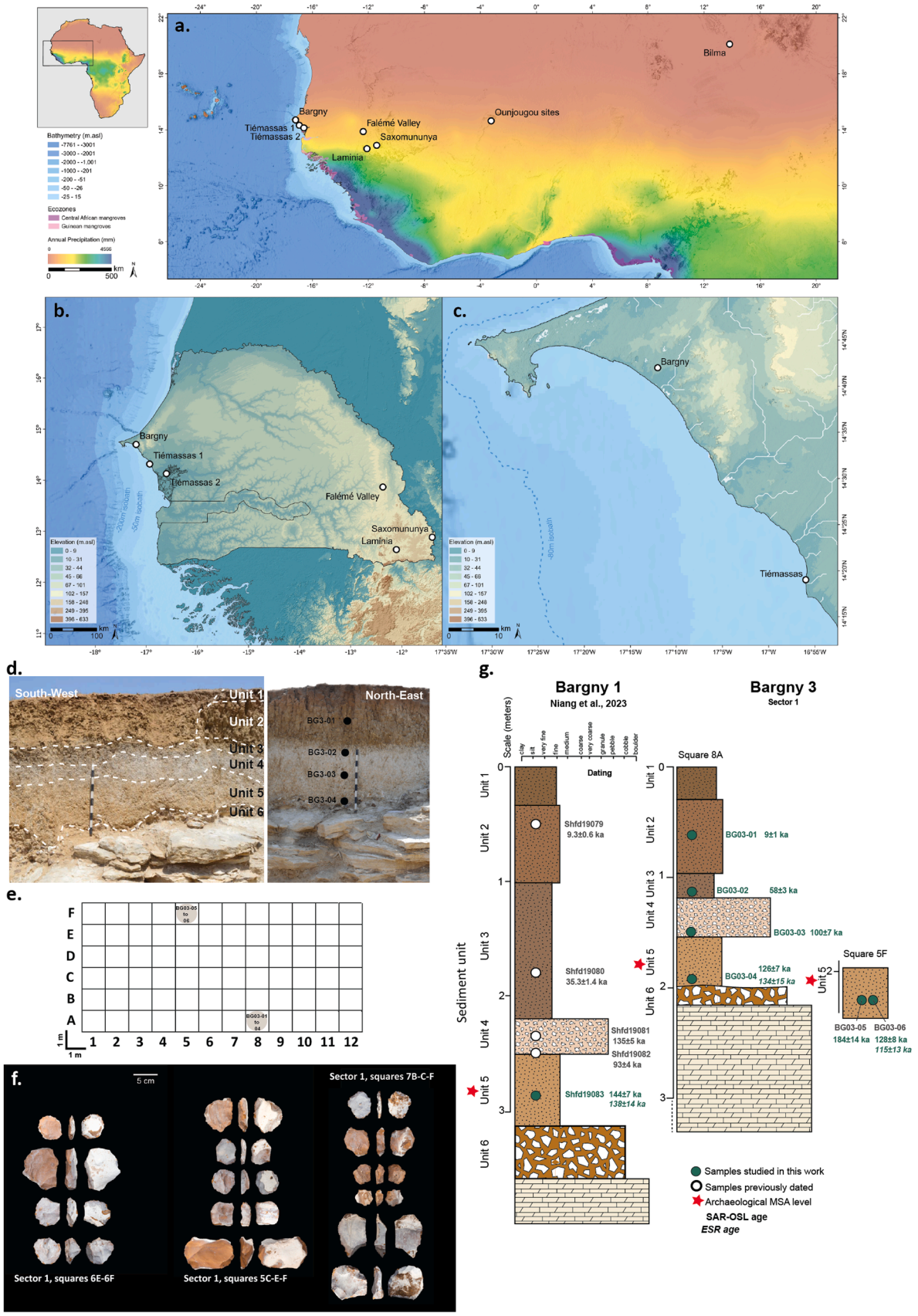

Fig. 1. Geographical location of the MSA sites presented and discussed in this work and Bargny 1 and 3 sequences. a: Location of the sites at west African scale and at b: regional scale; c: Location of Bargny sequences; d: View of the main sections of Bargny 3 without and with the OSL-ESR samples; e. Plan of Bargny 3 presenting the location of the dating samples in this work; f: Example of MSA artifacts from Unit 5 of Bargny 3; g: Stratigraphic sections of Bargny 1 and 3, and associated dating results. Data in (a-c) from ALOS (JAXA), GEBCO 2023 Grid, WorldClim 2.1 (bio12; Fick et al., 2017), and WWF (Dinerstein et al., 2017; Olson et al., 2001).

initially carried out in 2018, prior to the complete destruction of the site through quarrying activities, and no *in situ* measurements of the natural radioactivity was performed at that time. Consequently, no field gamma dose rate was available for the trapped charge-dating study initiated a few years later (Table S1).

Samples are stratigraphically distributed as follows, from top to bottom (Fig. 1): one was taken from each Unit 2, 3 and 4, while three samples originate from the lowermost Unit 5. The multiple sampling from the MSA horizon (Unit 5) aims to account for possible lateral variability of the ages and to evaluate the potential influence of post-depositional formation of carbonates that dominate the overlying Unit 4 deposits. Additionally, one prepared quartz sample (Shfd19083) from Unit 5 of Bargny 1 was also selected for ESR dating. The corresponding OSL age of 150±6 ka initially constrained the MSA Unit 5 to the latest part of the Middle Pleistocene (Niang et al., 2023).

The carbonate content of the six Bargny 3 samples has been determined at CENIEH (Burgos, Spain) using a Petron Calcimeter on ~5 g of dry, ground and homogenized sediments in order to quantify their impact on the dose rate and OSL-ESR ages (see Supplementary Material S1). Additionally, one thin section was made from sample BG03–04 (Unit 5) following the protocol detailed in Supplementary Material S2.

OSL dating of the six samples from Bargny 3 was performed following the Single Aliquot Regenerative (SAR) Dose protocol (Murray and Wintle, 2003), which is the same procedure previously used to date the Unit 5 of Bargny 1 (Niang et al., 2023). ESR dating was performed on three quartz samples (BG03–04 and BG05–06 from Bargny 3, and Shfd19083 from Bargny 1) using the multiple-centre (MC) approach (Toyoda et al., 2000), with the dose evaluation based on the Multiple Aliquot Additive Dose (MAAD) method. Three radiation-induced ESR signals (Al, Ti-mix and Ti-H) were systematically evaluated in each quartz sample. OSL and ESR dating analyses were carried out at CENIEH, following the procedures extensively described in Supplementary Material S1.

4. Results and discussion

A detailed discussion about the evaluation of the equivalent dose and dose rate for ESR and OSL methods, as well as of the reliability of the age results may be found in Supplementary Material S1.

4.1. Comparison of OSL and ESR dating results

4.1.1. Bargny 3

The final OSL and ESR results are presented in Table 1 and displayed in Fig. 2. The OSL ages range from 187±14 ka to 9±1 ka and are stratigraphically consistent. More specifically, Unit 5 shows two samples with close results around 130 ka (126±7 and 128±8 ka), while the third age is significantly older (BG03–05: 187±14 ka). Since the three samples show very close OSL D_e values (103±4, 110 ± 6 and 108±5 Gy), the apparent age scatter is most likely related to the dose rate evaluation (See Supplementary Material for an extended discussion). We do acknowledge that the absence of *in situ* dosimetry for Unit 5 may induce an intrinsic uncertainty on the gamma dose rate calculated for these samples, which can, however, hardly be quantified with the existing data set (see Supplementary Material). For example, one sample (BG03–04) is located within 30 cm of Unit 6 and has likely received a contribution from that unit and the bedrock. Moreover, sample BG03–05 shows the lowest total dose rate (586±26 μGy/a) of all samples, which systematically return values > 800 μGy/a (Table 1, Fig. 2). Interestingly, this sample not only shows the lower radionuclide concentrations (Table S4), but also a significant disequilibrium in the U-238 decay chain (Table S5) and by far the highest carbonate content (59 %; Table S6). Taking into account the disequilibrium may lead to the evaluation of a much lower dose rate, resulting in an age of 156±11 ka (Table S7; i.e., 30 ka younger than the initial age estimate of 187±14 ka). Moreover, micromorphological study of sample BG03–04 indicates that the formation of these carbonates is most likely post-depositional (Supplementary Material), which may potentially bias the dose rate evaluation (Nathan and Mauz, 2008). Dose rate modeling using RCarb software (Nathan and Mauz, 2008) suggests that the presence of carbonate may induce a dose rate overestimation of about 14 % if not taken into account Supplementary Material. An extended version of the discussion may be found in Supplementary Material S2. Consequently, there is evidence indicating that the older age initially obtained from BG03–05 is most likely strongly overestimated.

To sum up, the age of Unit 5 from Bargny 3 is therefore best estimated by the other two samples, from which a mean OSL age of 127±8 ka may be proposed, correlating the deposits to around the MIS 6–5 transition (130 ka, Lisiecki and Raymo, 2005).

MC ESR ages obtained for two samples from Unit 5 show the usual pattern indicating that Al and Ti-mix signals have not been fully reset

Table 1
Detailed OSL-ESR ages estimates and dose rate components. Errors are displayed at 1 sigma. The dose rate and OSL age of sample Shfd19083 have been recalculated to ensure a direct comparability with the ESR age (see text in Supplementary Material S1): the dose rate initially calculated by Niang et al. (2023) is given in brackets. Final OSL and ESR ages are in bold.

Sequence	**Bargny 3**						**Bargny 1**
Sample	**BG03-01 (Unit 2)**	**BG03-02 (Unit 3)**	**BG03-03 (Unit 4)**	**BG03-04 (Unit 5)**	**BG03-05 (Unit 5)**	**BG03-06 (Unit 5)**	**Shfd19083 (Unit 5)**
Depth (m)	0.62±0.1	1.15±0.1	1.55±0.1	1.95±0.1	2.34±0.1	2.34±0.1	3.1±0.1
Measured water (MW) content (dry weight %)	3.2±5	2.8±5	2.2±5	2.6±5	1.6±5	2.8±5	2.5±5
Internal dose rate (μGy/a)	30±1	30±1	30±1	30±1	30±1	30±1	30±1
Alpha dose rate (μGy/a)	7±5	9±6	6±5	6±4	4±3	6±5	12±9
Beta dose rate (μGy/a)	311±21	424±28	349±21	283±19	189±13	301±20	317±23
Gamma dose rate (μGy/a)	406±25	469±28	349±21	343±21	213±13	357±21	379±29
Cosmic dose rate (μGy/a)	191±19	173±17	164±16	156±16	149±15	149±15	136±14
Total dose rate (μGy/a)	946±39	1104±45	839±35	818±34	586±26	844±35	874±41 (840±33)
OSL D_e (Gy)	8±1	64±2	84±5	103±4	110±4	108±5	126±2
OSL Age (ka)	**9±1**	**58±3**	**100±7**	**126±7**	187±14	**128±8**	**144±7**
D_e (Gy) Al				140±17		148±14	185±16
D_e (Gy) Ti-mix (SSE W−1/I²; Dmax=2.5 kGy)				130±6		130±6	201±25
D_e (Gy) Ti-H (SSE W−1/I²; Dmax=2.5 kGy)				110±11		97±10	110±11
Age (ka) Al				171±22		175±18	212±12
Age (ka) Ti-mix (SSE W−1/I², D_{max}=2.5 kGy)				159±10		154±10	230±31
Age (ka) Ti-H (SSE W−1/I², D_{max}=2.5 kGy)				**134±15**		**115±13**	**138±14**
				Unit 5 OSL mean age of 127±8 ka			
				Unit 5 Ti-H ESR mean age of 125±14 ka			

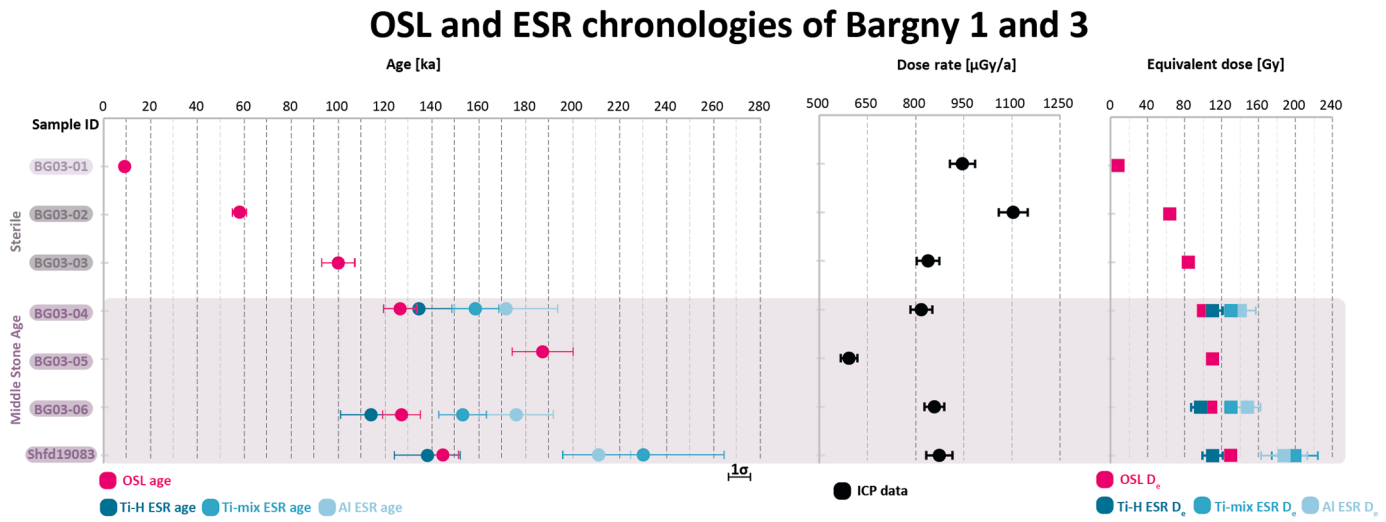

Fig. 2. Overview of the OSL-ESR data (ages, dose rate and equivalent dose) collected from Bargny 1 and 3 sequences. Numerical values are given in Table 1. Errors are 1σ.

during transport (see complete discussion in Supplementary Material S1), and the ages should therefore be regarded as maximum estimates. Consequently, the true age of the samples is best estimated by the Ti-H signal, which yields two 1σ-consistent results of 115 ± 13 ka (BG03–06) and 134±15 ka (BG03–04). These results are also in close agreement with the paired OSL age estimates. A mean Ti-H ESR age of 125±14 ka may therefore be calculated for Unit 5.

In summary, a robust chronostratigraphic framework may be established for Bargny 3 through a combination of OSL and ESR dating methods. OSL yields a stratigraphically-consistent chronology for the sedimentary sequence ranging from 9±1 ka at the top to 127±8 ka at the bottom, while the results obtained for lowermost Unit 5 (127±8 ka) are confirmed by the semi-independent age control given by the ESR, providing a very close age of 125±14 ka.

4.1.2. *Unit 5 from Bargny 1*

The new dose rate evaluation carried out for Shfd19083 from Unit 5 at Bargny 1 yields a revised OSL age of 144±7 ka (Supplementary Material S1), i.e., slightly lower by 6 ka than the initial age of 150±6 ka (Table 1; Niang et al., 2023). The limited D_e overdispersion (OD) of 11 % suggested that the sediment has been well bleached and limiting the risk to overestimate the true OSL age of the Unit 5. As for Bargny 3 samples, the ESR data indicate that the Al and Ti-mix signals have most likely not been fully reset, providing thus, in accordance with the MC approach (Toyoda et al., 2000), maximum age constraints of 212±12 ka and 230±31 ka, respectively. In contrast, the Ti-H signal returns a younger age of 138±14 ka, in excellent agreement with the semi-independent OSL age of 144±7 ka. In other words, both dating methods yield highly consistent ages of around 140 ka, confirming the deposition of Unit 5 at Bargny 1 may be correlated to the end of MIS 6 (191–130 ka; all MIS age boundaries used in this work are from Lisiecki and Raymo, 2005).

4.2. *Chronostratigraphic interpretation*

Our study documents and dates evidence for protohistoric and MSA occupations at Bargny 3, and fits the previously reported MSA occupation at Bargny 1 into an extended multi-methods geochronological framework based on OSL and ESR dating methods.

4.2.1. *Units 1–4*

The OSL results obtained for Unit 2 of Bargny 3 and Bargny 1 sequences are consistent, with similar ages of 8±1 ka (this work; Table 1) and 9±1 ka (Niang et al., 2023; Fig. 1). This suggests the modern configuration of the sedimentary landscape at Bargny was established in the early Holocene, which was subsequently occupied by later prehistoric and protohistoric populations as evidenced by shells, human burial, numerous charcoals and pottery fragments from the upper Unit 1 at both sites.

The sharp sediment boundary between Unit 2 and 3, as well as coarser sands in Unit 2 identified at Bargny 1, likely points towards an erosive event, that may have reshaped the contemporaneous landscape at Bargny, though the destruction of both the Bargny 1 and 3 sequences prohibits any further detailed assessment. The OSL age estimates for Unit 3 span 35.3±1.4 ka at Bargny 1–58±3 ka at Bargny 3, suggesting little change in depositional environments during much of MIS 3 (57–29 ka).

The age estimates for the underlying of Unit 4 of 100±7 ka at Bargny 3 falls within the range of the OSL results from Bargny 1 (134±5 ka and 90±4 ka). While we cannot exclude that the age scatter may partly result from the uncertainty on the dose rate evaluation (e.g., absence of in situ dosimetry at both sites; no data on carbonate content or about a potential disequilibrium in the U-238 for the Bargny 1 samples), these results nevertheless show overall good consistency across sites, and enable to roughly correlate Unit 4 to MIS 5 (130–71 ka).

4.2.2. *Unit 5*

There is approximately a 10–20 ka age difference between the numerical dating results obtained for Unit 5 at Bargny 1 and Bargny 3. While this may be partly explained by some minor uncertainty related with the dose rate evaluation of the Bargny 1 sample (i.e., the carbonate content and disequilibrium in the U-238 chain could not be assessed), or with the absence of *in situ* dosimetry at both sites, it may also naturally result from the non-negligible time span covered by sediment deposition of Unit 5. Regardless, it should be emphasized that the combined ESR-OSL dating results from the two sites are consistent at a 2σ confidence level. Based on the current data set available, it may therefore be reasonably considered that Units 5 at Bargny 1 and Bargny 3 may be coeval and represent the same depositional episode, with an age centred on 136±15 ka (2σ). This result provides an indirect age constraint to the associated MSA lithic assemblage, corroborating the occupation along the Senegambian coast spanning the MIS 6-MIS 5 transition. Consequently, the association of the MSA artifacts with estuarine and mangrove environments in the Senegalese coastline that was initially identified from the palaeoecological study of Unit 5 from Bargny 1 (Niang et al., 2023) may be reasonably extended to Bargny 3.

5. Conclusion

Together with Tiémassas sites (Niang et al., 2020, 2018), Bargny offers a unique opportunity to further evaluate the importance of the coast to Pleistocene populations in West Africa, which has been barely investigated so far, unlike in other parts of the continent (e.g. see synthesis in Ben Arous et al., 2024; Kandel et al., 2023). The results of the present work contribute to geographically and chronologically extend and enhance the resolution of the MSA record in West Africa, with sites located from the Senegalese coastline to inland regions such as the Ounjougou and the Falémé Valley sites (Chevrier et al., 2018; Rasse et al., 2020, 2012) and dated from the earliest MIS 5 to MIS 2. Interestingly, our results also bring additional complexity to our understanding of the early human dispersals into West Africa by suggesting that Bargny MSA occupations chronologically overlap with those at Ravin Blanc I (Falémé Valley sites, Fig. 1 **and** Fig. 3**).** The latter has indeed provided a very distinct lithic assemblage made of a mixture of MSA with Acheulean handaxes, which has been dated from 124±12 ka to 128±12 ka, and is associated with an open and humid environment (Douze et al., 2021).

Finally, the present work may also have significant methodological implications. First, the results confirm the great potential of the Ti-H ESR signal to date late Middle to Late Pleistocene quartz samples. Moreover, the excellent agreement obtained between the two semi-independent methods shows the usefulness of the combined OSL-ESR dating approach to establish robust chronologies for the MSA record of West Africa.

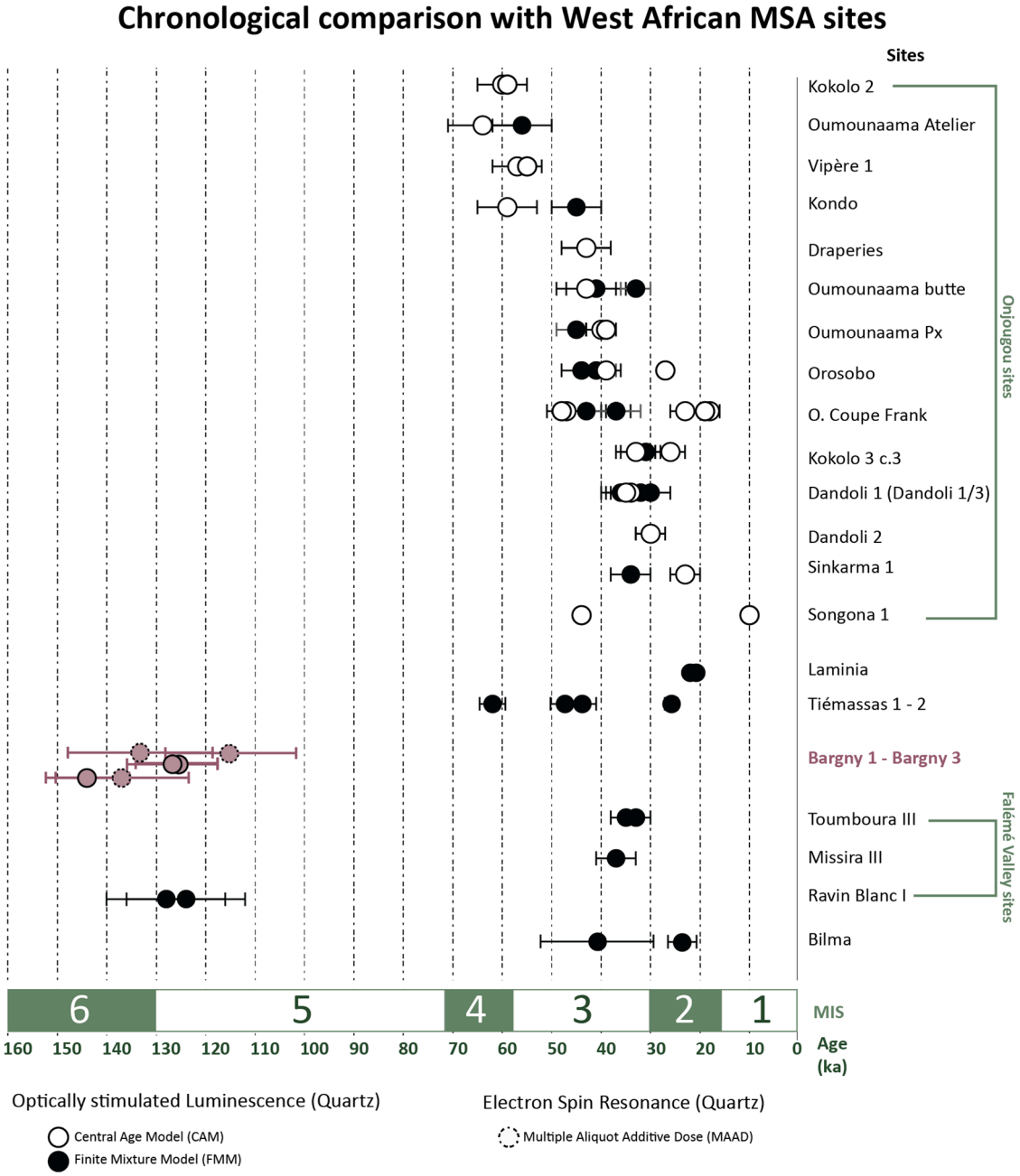

Fig. 3. The chronology of the MSA from Bargny 1 and 3 sequences compared to others MSA sites in West Africa dated by OSL. Site locations may be found in Fig. 1. The MSA OSL and Ti-H ESR dates obtained in this work are in purple. The OSL dates from comparative sites are from Niang et al. (2023); Douze et al. (2021); Chevrier et al. (2018). Errors are 1σ.

Declaration of Competing Interest

The authors declare that they have no known competing financial interests or personal relationships that could have appeared to influence the work reported in this paper.

Acknowledgements

Eslem Ben Arous' postdoctoral research has received funding from the Fyssen Foundation, the Max Planck Society (Human Palaeosystems Group), and the European Union's Horizon 2020 research and innovation programme under the Marie Skłodowska-Curie grant agreement No 101107408. Mathieu Duval's investigation is currently supported by the Spanish Ramón y Cajal Fellowship RYC2018–025221-I, which is funded by MCIN/AEI/ 10.13039/501100011033 and by 'ESF Investing in your future'. Khady Niang has received funding from European Union's Horizon 2020 research and innovation programme under the Marie Skłodowska-Curie grant agreement No 1010227259. Aspects of the work carried out by various co-authors (MdV, ACC, JIC, CS and MD) received support from Grant PID2021-123092NB-C22 funded by MCIN/AEI/ 10.13039/501100011033/FEDER, UE, and by "ERDF A way of making Europe". We also wish to thank Chantal Tribolo for performing and helping on the HRGS analyses at Archeosciences Bordeaux. We also would like to thank Sebastian Kreutzer and Barbara Mauz for their help with the use of RCarb package. We are grateful to anonymous reviewers for providing feedback on this manuscript.

Author contributions

The project was conceived by KN and implemented by EBA, JB and KN. KN and JB led excavations, cleaning and sampling. EMLS provided advice and guidance. EBA, MD, MdV, AM, MJAE and ACC conducted dating analyses. CC, CS and JIC were involved in the carbonates analyses and thin section. EBA coordinated and led the writing of the paper. EBA and AFB were responsible for drawing and compiling the illustrations. All authors contributed to the writing of the paper.

Appendix A. Supporting information

Supplementary data associated with this article can be found in the online version at doi:10.1016/j.qeh.2024.100044.

References

Bartz, M., Arnold, L.J., Demuro, M., Duval, M., King, G.E., Rixhon, G., Álvarez Posada, C., Parés, J.M., Brückner, H., 2019. Single-grain TT-OSL dating results confirm an Early Pleistocene age for the lower Moulouya River deposits (NE Morocco). Quat. Geochronol. 49, 138–145. https://doi.org/10.1016/J.QUAGEO.2018.04.007.

Bartz, M., Rixhon, G., Duval, M., King, G.E., Álvarez Posada, C., Parés, J.M., Brückner, H., 2018. Successful combination of electron spin resonance, luminescence and palaeomagnetic dating methods allows reconstruction of the Pleistocene evolution of the lower Moulouya river (NE Morocco). Quat. Sci. Rev. 185, 153–171. https://doi.org/10.1016/J.QUASCIREV.2017.11.008.

Ben Arous, E., Boisard, S., Leplongeon, A., 2024. The Upper Pleistocene Archaeology of northern Africa (Middle and Later Stone Age, from the western Maghreb to the Nile Valley). Encycl. Quat. Sci. 3e. p. forthcoming.

Ben Arous, E., Philippe, A., Shao, Q., Richter, D., Lenoble, A., Mercier, N., Richard, M., Stoetzel, E., Tombret, O., El Hajraoui, M.A., Nespoulet, R., Falguères, C., 2022. An improved chronology for the Middle Stone Age at El Mnasra cave, Morocco. PLoS One 17, 1–28. https://doi.org/10.1371/journal.pone.0261282.

Brooks, A.S., Yellen, J.E., Potts, R., Behrensmeyer, A.K., Deino, A.L., Leslie, D.E., Ambrose, S.H., Ferguson, J.R., D'Errico, F., Zipkin, A.M., Whittaker, S., Post, J., Veatch, E.G., Foecke, K., Clark, J.B., 2018. Long-distance stone transport and pigment use in the earliest Middle Stone Age. Sci. (80-.) 360, 90–94. https://doi.org/10.1126/science.aao2646.

Campmas, E., 2017. Integrating human-animal relationships into new data on aterian complexity: a paradigm shift for the North African Middle Stone Age. Afr. Archaeol. Rev. 34, 469–491. https://doi.org/10.1007/s10437-017-9273-z.

Caruana, M.V., Wilson, C.G., Arnold, L.J., Blackwood, A.F., Demuro, M., Herries, A.I.R., 2023. A marine isotope stage 13 Acheulian sequence from the Amanzi Springs Area 2 Deep Sounding excavation, Eastern Cape, South Africa. J. Hum. Evol. 176, 103324. https://doi.org/10.1016/J.JHEVOL.2023.103324.

Chevrier, B., Huysecom, Soriano, S., Rasse, M., Lespez, L., Lebrun, B., Tribolo, C., 2018. Between continuity and discontinuity: an overview of the West African Paleolithic over the last 200,000 years. Quat. Int. 466, 3–22. https://doi.org/10.1016/j.quaint.2017.11.027.

Daujeard, C., Falguères, C., Shao, Q., Geraads, D., Hublin, J.-J., Lefèvre, D., Graoui, M., El, Rué, M., Gallotti, R., Delvigne, V., Queffelec, A., Arous, E.Ben, Tombret, O., Mohib, A., Raynal, J.-P., 2020. Earliest African evidence of carcass processing and consumption in cave at 700 ka, Casablanca, Morocco. Sci. Rep. 2020 101 10, 1–15. https://doi.org/10.1038/s41598-020-61580-4.

Deino, A.L., Behrensmeyer, A.K., Brooks, A.S., Yellen, J.E., Sharp, W.D., Potts, R., 2018. Chronology of the acheulean to middle stone age transition in eastern Africa. Sci. (80-.) 360, 95–98. https://doi.org/10.1126/SCIENCE.AAO2216.

Dinerstein, E., Olson, D., Joshi, A., Vynne, C., Burgess, N.D., Wikramanayake, E., Hahn, N., Palminteri, S., Hedao, P., Noss, R., Hansen, M., Locke, H., Ellis, E.C., Jones, B., Barber, C.V., Hayes, R., Kormos, C., Martin, V., Crist, E., Sechrest, W., Price, L., Baillie, J.E.M., Weeden, D., Suckling, K., Davis, C., Sizer, N., Moore, R., Thau, D., Birch, T., Potapov, P., Turubanova, S., Tyukavina, A., De Souza, N., Pintea, L., Brito, J.C., Llewellyn, O.A., Miller, A.G., Patzelt, A., Ghazanfar, S.A., Timberlake, J., Klöser, H., Shennan-Farpón, Y., Kindt, R., Potapov, J.P.B., Van Breugel, P., Graudal, L., Voge, M., Al-Shammari, K.F., Saleem, M., 2017. An Ecoregion-Based Approach to Protecting Half the Terrestrial Realm. Bioscience 67, 534–545. https://doi.org/10.1093/biosci/bix014.

Diop, A., 1976. Contribution à la Connaissance des Industries Paléolithiques Post-Acheuléennes dans la Presquîle du Cap-Vert. Université Cheikh Anta Diop de Dakar.

Douze, K., Lespez, L., Rasse, M., Tribolo, C., Garnier, A., Lebrun, B., Mercier, N., Ndiaye, M., Chevrier, B., Huysecom, E., 2021. A West African Middle Stone Age site dated to the beginning of MIS 5: Archaeology, chronology, and paleoenvironment of the Ravin Blanc I (eastern Senegal). J. Hum. Evol. 154, 102952. https://doi.org/10.1016/j.jhevol.2021.102952.

Duval, M., Arnold, L.J., Demuro, M., Parés, J.M., Campaña, I., Carbonell, E., Bermúdez de Castro, J.M., 2022. New chronological constraints for the lowermost stratigraphic unit of Atapuerca Gran Dolina (Burgos, N Spain). Quat. Geochronol. 71. https://doi.org/10.1016/j.quageo.2022.101292.

Duval, M., Sahnouni, M., Parés, J.M., van der Made, J., Abdessadok, S., Harichane, Z., Cheheb, R.C., Boulaghraif, K., Pérez-González, A., 2021. The Plio-Pleistocene sequence of Oued Boucherit (Algeria): A unique chronologically-constrained archaeological and palaeontological record in North Africa. Quat. Sci. Rev. 271. https://doi.org/10.1016/j.quascirev.2021.107116.

Fick, S.E., Hijmans, R.J., 2017. WorldClim 2: new 1-km spatial resolution climate surfaces for global land areas. Int. J. Climatol. 37, 4302–4315. https://doi.org/10.1002/JOC.5086.

Herries, A.I.R., Curnoe, D., Adams, J.W., 2009. A multi-disciplinary seriation of early Homo and Paranthropus bearing palaeocaves in southern Africa. Quat. Int. 202, 14–28. https://doi.org/10.1016/J.QUAINT.2008.05.017.

Hublin, J.-J., Ben-Ncer, A., Bailey, S.E., Freidline, S.E., Neubauer, S., Skinner, M.M., Bergmann, I., Le Cabec, A., Benazzi, S., Harvati, K., Gunz, P., 2017. New fossils from Jebel Irhoud, Morocco and the pan-African origin of Homo sapiens. Nature 546, 289–292. https://doi.org/10.1038/nature22336.

Kandel, A.W., Sommer, C., Kanaeva, Z., Bolus, M., Bruch, A.A., Groth, C., Haidle, M.N., Hertler, C., Heß, J., Malina, M., Mä rker, M., Hochschild, V., Mosbrugger, V., Schrenk, F., Conard, N.J., 2023. The ROCEEH Out of Africa Database (ROAD): A large-scale research database serves as an indispensable tool for human evolutionary studies. ⟨https://doi.org/10.1371/journal.pone.0289513⟩.

Lebrun, B., Tribolo, C., Chevrier, B., Rasse, M., Lespez, L., Leplongeon, A., Hajdas, I., Camara, A., Mercier, N., Huysecom, É., 2016. Establishing a West African chrono-cultural framework: First luminescence dating of sedimentary formations from the Falémé Valley, Eastern Senegal. J. Archaeol. Sci. Rep. 7, 379–388. https://doi.org/10.1016/J.JASREP.2016.05.001.

Lisiecki, L.E., Raymo, M.E., 2005. A Pliocene-Pleistocene stack of 57 globally distributed benthic Delta18O records. Paleoceanography 20, 1–17. https://doi.org/10.1029/2004PA001071.

Méndez-Quintas, E., Santonja, M., Pérez-González, A., Duval, M., Demuro, M., Arnold, L. J., 2018. First evidence of an extensive Acheulean large cutting tool accumulation in Europe from Porto Maior (Galicia, Spain). Sci. Rep. 8. https://doi.org/10.1038/s41598-018-21320-1.

Murray, A.S., Wintle, A.G., 2003. The single aliquot regenerative dose protocol: potential for improvements in reliability. Radiat. Meas. 37, 377–381. https://doi.org/10.1016/S1350-4487(03)00053-2.

Nathan, R.P., Mauz, B., 2008. On the dose-rate estimate of carbonate-rich sediments for trapped charge dating. Radiat. Meas. 43, 14–25. https://doi.org/10.1016/J.RADMEAS.2007.12.012.

Niang, K., Blinkhorn, J., Bateman, M.D., Kiahtipes, C.A., 2023. Longstanding behavioural stability in West Africa extends to the Middle Pleistocene at Bargny, coastal Senegal. Nat. Ecol. Evol. 2023, 1–11. https://doi.org/10.1038/s41559-023-02046-4.

Niang, K., Blinkhorn, J., Ndiaye, M., 2018. The oldest Stone Age occupation of coastal West Africa and its implications for modern human dispersals: new insight from Tiémassas. Quat. Sci. Rev. https://doi.org/10.1016/j.quascirev.2018.03.022.

Niang, K., Blinkhorn, J., Ndiaye, M., Bateman, M., Seck, B., Sawaré, G., 2020. The Middle Stone Age occupations of Tiémassas, coastal West Africa, between 62 and 25 thousand years ago. J. Archaeol. Sci. Rep. 34, 102658. https://doi.org/10.1016/J.JASREP.2020.102658.

Olson, D.M., Dinerstein, E., Wikramanayake, E.D., Burgess, N.D., Powell, G.V.N., Underwood, E.C., D'Amico, J.A., Itoua, I., Strand, H.E., Morrison, J.C., Loucks, C.J., Allnutt, T.F., Ricketts, T.H., Kura, Y., Lamoreux, J.F., Wettengel, W.W., Hedao, P., Kassem, K.R., 2001. Terrestrial ecoregions of the world: A new map of life on Earth.

Bioscience 51, 933–938. https://doi.org/10.1641/0006-3568(2001)051[0933:TEOTWA]2.0.CO;2.

Rasse, M., Lespez, L., Lebrun, B., Tribolo, C., Chevrier, B., Douze, K., Garnier, A., Davidoux, S., Hadjas, I., Ollier, C., Camara, A., Ndiaye, M., Huysecom, E., 2020. Synthèse morpho-sédimentaire et occurences archéologiques dans la vallée de la Falémé (de 80 à 5 ka; Sénégal oriental): mise en évidence d'une permanence des occupations à la transition Pléistocène-Holocène. Quaternaire 71–88. https://doi.org/10.4000/quaternaire.13181.

Rasse, M., Tribolo, C., Soriano, S., Huysecom, E., 2012. Premières données chronostratigraphiques sur les formations du Pléistocène supérieur de la « falaise » de Bandiagara (Mali, Afrique de l'Ouest). http://journals.openedition.org/quaternaire 23, 5–23. https://doi.org/10.4000/QUATERNAIRE.6163.

Richter, D., Grün, R., Joannes-Boyau, R., Steele, T.E., Amani, F., Rué, M., Fernandes, P., Raynal, J.-P., Geraads, D., Ben-Ncer, A., Hublin, J.-J., McPherron, S.P., 2017. The age of the hominin fossils from Jebel Irhoud, Morocco, and the origins of the Middle Stone Age. Nature 546, 293–296. https://doi.org/10.1038/nature22335.

Scerri, E., 2017. The North African Middle Stone Age and its place in recent human evolution. Evol. Anthropol. 26, 119–135. https://doi.org/10.1002/evan.21527.

Scerri, E.M.L., Niang, K., Candy, I., Blinkhorn, J., Mills, W., Cerasoni, J.N., Bateman, M. D., Crowther, A., Groucutt, H.S., 2021. Continuity of the Middle Stone Age into the Holocene. Sci. Rep. 11, 70. https://doi.org/10.1038/s41598-020-79418-4.

Scerri, E.M.L., Thomas, M.G., Manica, A., Gunz, P., Stock, J.T., Stringer, C., Grove, M., Groucutt, H.S., Timmermann, A., Rightmire, G.P., D'Errico, F., Tryon, C.A., Drake, N.A., Brooks, A.S., Dennell, R.W., Durbin, R., Henn, B.M., Lee-Thorp, J., DeMenocal, P., Petraglia, M.D., Thompson, J.C., Scally, A., Chikhi, L., 2018. Did our species evolve in subdivided populations across Africa, and why does it matter? Trends Ecol. Evol. 33, 582–594. https://doi.org/10.1016/j.tree.2018.05.005.

Schmid, Viola C., Douze, K., Tribolo, Chantal, Lorenzo Martinez, M., Rasse, Michel, Lespez, Laurent, Lebrun, Brice, Hérisson, David, Ndiaye, M., Huysecom, Eric, Schmid, V.C., Douze, K., Huysecom, E., Tribolo, C., Lebrun, B., Lebrun, B., Martinez, M.L., Rasse, M., Lespez, L., Hérisson, D., 2021. Middle Stone Age bifacial technology and pressure flaking at the MIS 3 site of toumboura III, eastern senegal. Afr. Archaeol. Rev. https://doi.org/10.1007/s10437-021-09463-5.

Shipton, C., Roberts, P., Archer, W., Armitage, S.J., Bita, C., Blinkhorn, J., Courtney-Mustaphi, C., Crowther, A., Curtis, R., Errico, F. d', Douka, K., Faulkner, P., Groucutt, H.S., Helm, R., Herries, A.I.R., Jembe, S., Kourampas, N., Lee-Thorp, J., Marchant, R., Mercader, J., Marti, A.P., Prendergast, M.E., Rowson, B., Tengeza, A., Tibesasa, R., White, T.S., Petraglia, M.D., Boivin, N., 2018. 78,000-year-old record of Middle and Later stone age innovation in an East African tropical forest. Nat. Commun. 9, 1832. https://doi.org/10.1038/s41467-018-04057-3.

Smith, E.I., Jacobs, Z., Johnsen, R., Ren, M., Fisher, E.C., Oestmo, S., Wilkins, J., Harris, J.A., Karkanas, P., Fitch, S., Ciravolo, A., Keenan, D., Cleghorn, N., Lane, C.S., Matthews, T., Marean, C.W., 2018. Humans thrived in South Africa through the Toba eruption about 74,000 years ago. Nat 2018 5557697 555, 511–515. https://doi.org/10.1038/nature25967.

Toyoda, S., Voinchet, P., Falgueres, C., Dolo, J.-M., Laurent, M., 2000. Bleaching of ESR signals by the sunlight: a laboratory experiment for establishing the ESR dating of sediments. Appl. Radiat. Isot. 52, 1357–1362.

Tribolo, C., Mercier, N., Rasse, M., Soriano, S., Huysecom, E., 2010. Kobo 1 and L'Abri aux Vaches (Mali, West Africa): two case studies for the optical dating of bioturbated sediments. Quat. Geochronol. 5, 317–323. https://doi.org/10.1016/J.QUAGEO.2009.03.002.

Will, M., Kandel, A.W., Kyriacou, K., Conard, N.J., 2016. An evolutionary perspective on coastal adaptations by modern humans during the Middle Stone Age of Africa. Quat. Int. 404, 68–86. https://doi.org/10.1016/j.quaint.2015.10.021.